Multi-bit Decentralized Detection Through Fusing Smart & Dumb Sensors Based on Rao Test

X. Cheng, D. Ciuonzo, *Senior Member, IEEE*, and P. Salvo Rossi, *Senior Member, IEEE*

Abstract—We consider Decentralized Detection (DD) of an unknown signal corrupted by zero-mean unimodal noise via Wireless Sensor Networks (WSNs). We assume the presence of both smart and dumb sensors: the former transmit unquantized measurements, while the latter employ multi-level quantizations (before transmission through binary symmetric channels) in order to cope with energy and/or bandwidth constraints. The data are received by a Fusion Center (FC), which relies on a proposed Rao test, as a simpler alternative to the Generalized Likelihood Ratio Test (GLRT). The asymptotic performance analysis of the multi-bit Rao test is provided and exploited to propose a (signal-independent) quantizer design approach by maximizing the non-centrality parameter of the test-statistic distribution. Since the latter is a non-linear and non-convex function of the quantization thresholds, we employ the particle swarm optimization algorithm for its maximization. Numerical results are provided to show the effectiveness of Rao test in comparison to GLRT and the boost in performance obtained by (multiple) threshold optimization. Asymptotic performance is also exploited to define detection gain measures allowing to assess gain arising from (a) use of dumb sensors and (b) increasing their quantization resolution.

Index Terms—Decentralized detection, multilevel quantization, Rao test, threshold optimization, wireless sensor networks.

I. INTRODUCTION

A. Motivation and Related Works

DECENTRALIZED Detection (DD) via Wireless Sensor Networks (WSNs) has received significant attention by the scientific community over the last two decades [1]–[11]. A WSN with a centralized architecture typically consists of a large number of spatially-distributed sensors and a Fusion Center (FC). The sensors collect measurements of a given physical process (temperature, humidity, etc.) or, in case of DD, are in charge of detecting some specific events in a region of interest [12]. These may correspond to target/signal presence or anomalies, e.g. deviations from normal behavior attributed to unforeseen changes in the system/environment. Relevant applications for the aerospace field include detection of solar flares (big energy releases from the sun), cyber-attacks targeting the power grids [13], fault-detection in aircraft systems and inertial navigation systems, pervasive monitoring of critical infrastructures and (cooperative) spectrum exploitation

for aeronautical communications [14]. Collectively, a WSN is able to exploit spatial diversity similarly to multistatic [15] or distributed MIMO radars [16], [17].

Sensor nodes are usually subject to strict energy and/or bandwidth constraints and, therefore, they may be compelled to *quantize* their measurements, before reporting them to the FC. Therein, a final (improved) decision is made [18], [19] based on a corresponding *fusion rule*, which is object of design efforts. The simplest and coarsest compression is accomplished by a one-bit quantizer, namely the measurement statistic is compared to a single threshold. In DD case, it is well-known that the optimal per-sensor statistic (under Bayesian/Neyman-Pearson frameworks) corresponds to a one-bit quantization of the local Likelihood-Ratio (LR) [20], [21]. Unfortunately, incomplete knowledge of the parameters of the event to be detected precludes the sensors from computing local LRs. Additionally, the search for quantization thresholds is exponentially complex [2], thus the bit sent is either the result of a "dumb" quantization [22] or embodies the estimated binary event, based on a sub-optimal rule [23]. Also, since the signal model is only partially-known, the FC is faced either to learn the parameters adaptively [24] or to tackle a composite hypothesis test; in the latter case the Generalized LR Test (GLRT) is usually employed as the relevant fusion rule [19], [25]–[27].

Accordingly, in [19] DD of an unknown deterministic signal is tackled (i) based on one-bit quantizers, (ii) over error-prone reporting channels and (iii) via a GLRT at the FC. Differently, in [22], a one-bit Rao fusion rule is proposed as a simpler (from a computational viewpoint) alternative to the aforementioned one-bit GLRT. In both these works, threshold optimization was performed via their common (weak-signal) asymptotic performance and it has been shown that the optimal value corresponds to zero in many practical cases, except for some heavy-tailed distributions, such as the Generalized Gaussian Distribution (GGD). Similar findings, referring however to a decentralized estimation problem, were later obtained in [28]. More recently, a detailed study on threshold optimization for one-bit DD in GGD noise has appeared in [29].

Remarkably, the one-bit DD problem considered in [19], [22] has been tackled in [30] under a sequential setup and a sequential version of the GLRT as been employed at the FC for revealing the event of interest. On the other hand, we remark that one-bit DD of an unknown random signal (with uncertain variance) has been also analyzed in the literature [11], [25], where similar composite hypothesis testing tools have been capitalized for fusion rules design and threshold

optimization. Finally, a generalized form of one-bit Rao test has been recently devised for DD of *uncooperative targets* [31] and threshold optimization achieved via a heuristic rationale.

Apparently, there is a noticeable performance gap between the one-bit detector and a detector using unquantized observations, due to the considerable amount of useful information lost for the DD task [19]. In this respect, *multi-level quantization* is sought to fill this gap by trading off performance and complexity.

In view of the aforementioned reasons, Gao et al. [26] have recently considered multi-bit DD of a signal parameter in *Gaussian noise* for multisensor fusion in WSNs, where a *non-closed form* (multi-bit) GLRT has been devised. Indeed, the aforementioned GLRT detector requires the evaluation of the Maximum Likelihood (ML) estimate of the unknown signal parameter [32], which cannot be obtained in closed form, thus increasing the computational complexity of its implementation. In the same work, a (weak-signal) asymptotically-optimal threshold set choice has been obtained, resorting to the popular Particle Swarm Optimization Algorithm (PSOA) [33]. Numerical results therein have demonstrated that 2- or 3-bit quantization is sufficient for the GLRT to approach the performance of its unquantized counterpart.

Additionally, we mention that a further realistic complication is represented by the need for fusing sensors with different quantization resolutions, and, in some cases, able to provide their unquantized analog data to the FC, as recently studied in [34], [35] for a decentralized estimation problem. The need for considering this type of sensors can be motivated by sensors being very close to the FC, then capable of transmitting their unquantized data with little cost in terms of battery depletion (as opposed to further sensor nodes, whose measurements need to be quantized). Taking into account quantized and unquantized measurements at the FC also well suits to modeling measurement fusion of human-originated (quantized) and sensors-originated (analog) measurements [34].

In the following, a sensor will be referred to as *dumb* (resp. *smart*) if it transmits a *quantized* (resp. *unquantized*) version of its observation.

B. Contributions and Paper Organization

The main contributions of this paper are summarized as follows:

- We study the problem of DD of a noise-corrupted unknown signal parameter in WSNs [19], [22], [26]. To cope with WSNs stringent energy and bandwidth budgets, we consider multi-level quantized (dumb) sensors and, additionally, we assume the quantized data to be transmitted through (error-prone) Binary Symmetric Channels (BSC) to a FC, similarly as in [26]. However, as opposed to [26], we *only constrain the noise to be zero-mean unimodal-symmetric*. Furthermore, to enrich and make our setup more flexible, the *presence of* unquantized measurements at the FC from *smart sensors* is also considered [34].
- To capitalize multi-level measurements and perform a global decision at the FC, we develop a computationally-simpler alternative fusion rule to the GLRT (analyzed in

[26] only for dumb sensors' case), based on the Rao test. The corresponding multi-bit Rao fusion rule comprises the one-bit counterpart in [22] as a *special case*, although it does not represent a trivial extension of the above simplified scenario, and represents an appealing method for capitalizing fusion of both smart and dumb sensors. Indeed, the main advantage is that it *does not require* any estimation procedure [36] and it is available in *closed-form* even in the considered general model.

- We provide the asymptotic (weak-signal) performance of Rao fusion rule. Leveraging its explicit expression, *first* we adopt a quantizer design approach for dumb sensors which aims at maximizing the corresponding *non-centrality parameter*. Since the objective function is nonlinear and non-convex in the quantization levels to be optimized, a gradient search is not effective (and a closed-form cannot be obtained, as in the simpler one-bit case [23]), and thus we resort to a PSOA, following [26]. *Secondly*, the asymptotic performance is capitalized to define (for the first time) asymptotic detection gains which concisely allow to assess the improvement on WSN system performance of (i) dumb sensors and (ii) increasing the bit resolution of dumb sensors.
- Finally, the Rao test is compared to the GLRT through simulations (pertaining to relevant Gaussian and Generalized Gaussian noise cases) showing that, in addition to sharing the same asymptotic distribution, it achieves practically the same performance for a finite number of sensors.

We highlight that the present work extends our earlier conference paper [37], which provided (i) only a *preliminary analysis* of the quantizer optimization based on PSOA, (ii) considered *only dumb sensors* and (iii) did not introduce asymptotic detection gains of Rao test (as well as GLRT) versus resolution.

The rest of the manuscript is organized as follows. Sec. II introduces the model whereas in Sec. III the multi-bit Rao test is derived; in Sec. IV an asymptotic analysis of the multi-bit Rao detector is presented, and the multilevel quantizers is designed by using the PSOA. Performance analysis versus resolution of quantization is investigated in Sec. V. Numerical results and comparisons are provided in Sec. VI. Finally, concluding remarks and further avenues of research are given in Sec. VII. Additional proofs are deferred to dedicated appendices.

Notation - Lower-case bold letters denote vectors, with a_n being the nth element of $\boldsymbol{a}$; upper-case calligraphic letters, e.g. $\mathcal{A}$, denote finite sets; $\mathbb{E}\{\cdot\}$, $\mathrm{var}\{\cdot\}$ and $(\cdot)^T$ denote expectation, variance and transpose, respectively; $P(\cdot)$ and $p(\cdot)$ are used to denote Probability Mass Functions (PMF) and Probability Density Functions (PDF), respectively, while $P(\cdot|\cdot)$ and $p(\cdot|\cdot)$ their corresponding conditional counterparts; $F(\cdot)$ is used to denote the Complementary Cumulative Distribution Function (CCDF); $\mathcal{N}(\mu, \sigma^2)$ denotes a Gaussian PDF with mean μ and variance σ^2; χ_k^2 (resp. $\chi_k^{'2}(\xi)$) denotes a chi-square (resp. a non-central chi-square) PDF with k degrees of freedom (resp. and non-centrality parameter ξ); $\mathcal{U}(a, b)$ denotes a uniform PDF with support $[a, b]$; $\mathcal{L}(\mu, \beta)$ denotes a Laplace PDF with mean μ and scale parameter β; $\mathcal{GN}(\mu, \alpha, \epsilon)$ denotes a

Generalized Normal PDF with mean μ, scale α and shape ϵ; $\mathcal{Q}(\cdot)$ denotes the CCDF of the standardized normal random variable and $\mathcal{Q}^{-1}(\cdot)$ is its inverse function; $\Gamma(x)$ and $\gamma[s,x]$ denote the complete and lower-incomplete Gamma functions, respectively; the symbols $\sim$ and $\overset{a}{\sim}$ mean "distributed as" and "asymptotically distributed as".

II. PROBLEM STATEMENT

The system model, depicted in Fig. 1, is described as follows. We consider a binary hypothesis test in which a set of K sensors, divided in K_q dumb sensors and K_u smart sensors, collaborate [34] to detect the presence of an *unknown deterministic* parameter $\theta \in \mathbb{R}$, associated to a Phenomenon Of Interest (POI).

The problem at each sensor can be summarized as follows

$$\begin{cases} \mathcal{H}_0 & : \quad x_k = w_k, \\ \mathcal{H}_1 & : \quad x_k = h_k\,\theta + w_k, \end{cases} \quad (1)$$

where $x_k \in \mathbb{R}$ denotes the kth sensor measurement, $h_k \in \mathbb{R}$ is a known observation coefficient and $w_k \in \mathbb{R}$ denotes the noise random variable (RV) with $\mathbb{E}\{w_k\} = 0$ and *unimodal symmetric* PDF, denoted with $p_{w_k}(\cdot)$ in what follows. These assumptions imply that the PDF is strictly increasing (resp. decreasing) before (resp. after) the mode value, also coinciding with the mean and the median, and being zero in this case[1]. Furthermore, the RVs w_k are assumed *mutually independent*, namely $p_{w_1,\cdots,w_K}(\cdot) = \prod_{k=1}^{K} p_{w_k}(\cdot)$. Consequently, it holds $\mathbb{E}[w_\ell\,w_k] = \mathbb{E}[w_\ell]\,\mathbb{E}[w_k] = 0$ for $\ell \neq k$. We observe that $w_1,\ldots,w_K$ statistical knowledge corresponds to a reliable estimation of the sensor noise PDF(s) based on past historical (training) data. Finally, it is worth noting that Eq. (1) refers to a *two-sided test* [36], where $\{\mathcal{H}_0, \mathcal{H}_1\}$ corresponds to $\{\theta = \theta_0, \theta \neq \theta_0\}$ (in our case $\theta_0 = 0$).

Sensors are indexed such that the first K_q are *dumb*, and the remaining K_u are *smart*, which are assumed to be linked to the FC through ideal (error-free) channels. In order to better differentiate the characteristics of dumb and smart sensors, we denote:

- $\boldsymbol{b}_k$ the (compressed) sensing data transmitted from the kth *dumb* sensor based on multi-level quantization of the observation x_k as described in the following, where $k = 1, 2, \ldots, K_q$;
- $s_\kappa = x_{K_q+\kappa}$ the (fine-grained) sensing data transmitted by the κth *smart* sensor, where $\kappa = 1, 2, \ldots, K_u$.

More specifically, we assume that the kth dumb sensor employs a (multi-level) $q(k)$-bit deterministic[2] quantizer, in which the observation x_k is compared with a set of quantization thresholds $\{\tau_k(i)\}_{i=0}^{2^{q(k)}}$, (being $\tau_k(0) \triangleq -\infty$ and $\tau_k(2^{q(k)}) \triangleq +\infty$ two "dummy" thresholds set for notational convenience), determining $2^{q(k)}$ non-overlapping quantization intervals covering the whole $\mathbb{R}$. Specifically, the corresponding quantizer output is encoded as a binary codeword denoted by

---

[1]This class of PDFs comprises many noteworthy examples, such as the Gaussian, Laplace, Cauchy and generalized Gaussian distributions [36].

[2]In this work we restrict our attention to deterministic quantizers for simplicity; the more general case of probabilistic quantizers [10], although interesting, falls beyond the scope of this paper.

$\boldsymbol{b}_k \in \{0,1\}^{q(k)}$, where $k = 1, 2, \ldots, K$. The non-overlapping quantization intervals are associated to $q(k)$-bit binary codewords $\boldsymbol{v}(i) = \begin{bmatrix} v_1(i) & \cdots & v_{q(k)}(i) \end{bmatrix}^T$, where $v_t(i) \in \{0,1\}$. Hence, the output codeword of $q(k)$-bit quantizer at the kth sensor can be expressed as:

$$\boldsymbol{b}_k \triangleq \begin{cases} \boldsymbol{v}(1) & -\infty < x_k < \tau_k(1) \\ \boldsymbol{v}(2) & \tau_k(1) \leq x_k < \tau_k(2) \\ \vdots & \vdots \\ \boldsymbol{v}(2^{q(k)}) & \tau_k(2^{q(k)} - 1) \leq x_k < +\infty \end{cases} \quad (2)$$

We observe that herein *raw measurement quantization* (as opposed to other local sensor processing, e.g. quantization of energy statistic [11]) is pursued to keep the signal polarity in case an estimate of θ is required after detection.

The codeword of kth (dumb) sensor is then transmitted to the FC over an error-prone reporting link, and the transmission process of *each bit* is modeled as an independent BSC with (known) Bit-Error Probability (BEP) $P_{e,k}$. The FC will then receive a distorted codeword $\boldsymbol{y}_k$ from kth sensor, whose conditional probability is:

$$P(\boldsymbol{y}_k = \boldsymbol{v}_k(i)|\boldsymbol{b}_k = \boldsymbol{v}_k(j)) = \underbrace{P_{e,k}^{d_{i,j}}\,(1 - P_{e,k})^{(q(k) - d_{i,j})}}_{\triangleq\,G_{q(k)}(P_{e,k}, d_{i,j})} \quad (3)$$

where $d_{i,j} \triangleq d(\boldsymbol{v}_k(i), \boldsymbol{v}_k(j))$ denotes the Hamming distance between codewords $\boldsymbol{v}_k(i)$ and $\boldsymbol{v}_k(j)$.

Remark: We highlight that the formulation pursued in this work allows for some useful generalizations, e.g. a more general channel (vector) transition (from codeword $\boldsymbol{v}(j)$ to $\boldsymbol{v}(i)$) probability expression. This could be simply achieved by replacing $G_{q(k)}(P_{e,k}, d_{i,j})$ (cf. Eq. (3)) with a more complicated functional $P_{e,k}(\boldsymbol{v}(i), \boldsymbol{v}(j))$, allowing to remove the assumption of independent BSC uses.

For the sake of notational convenience, we collect measurements sensed and transmitted by smart sensors in the vector $\boldsymbol{s} = \begin{bmatrix} s_1 & \cdots & s_{K_u} \end{bmatrix}^T \in \mathbb{R}^{K_u}$ whereas the noisy codewords (viz. soft-quantized measurements) received from the dumb sensors in the set $\boldsymbol{Y} \triangleq \{ \boldsymbol{y}_1 \; \cdots \; \boldsymbol{y}_{K_q} \}$ (recall that $\boldsymbol{y}_k \in \{0,1\}^{q(k)}$ and thus codewords from dumb sensors may differ in length).

The hybrid PDF/PMF of the observations $\{\boldsymbol{Y}, \boldsymbol{s}\}$ as a function of θ is then given by

$$p(\boldsymbol{Y}, \boldsymbol{s}; \theta) = \prod_{k=1}^{K_q} P(\boldsymbol{y}_k; \theta) \prod_{\kappa=1}^{K_u} p_{w_{K_q+\kappa}}(s_\kappa - h_{K_q+\kappa}\,\theta). \quad (4)$$

Clearly, $p(\boldsymbol{Y}, \boldsymbol{s}; \theta_0)$ denotes the hybrid PDF/PMF under $\mathcal{H}_0$. The corresponding PMF of the quantized and (channel-)distorted measurement from kth (dumb) sensor can be further expanded as

$$P(\boldsymbol{y}_k; \theta) = \sum_{i=1}^{2^{q(k)}} P(\boldsymbol{y}_k|\boldsymbol{b}_k = \boldsymbol{v}(i))\,P(\boldsymbol{b}_k = \boldsymbol{v}(i); \theta). \quad (5)$$
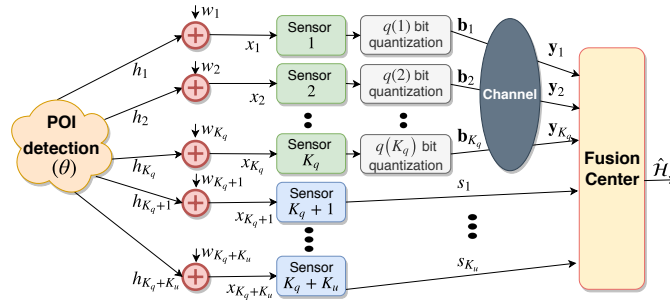
Fig. 1: WSN system model with dumb (multi-bit and error-prone) and smart (full-precision and error-free) sensors.

Based on the quantizer law reported in Eq. (2), the PMF $P(\boldsymbol{b}_k = \boldsymbol{v}(i); \theta)$ is given by

$$
\begin{aligned}
P(\boldsymbol{b}_k = \boldsymbol{v}(i); \theta) &= \Pr\{\tau_k(i-1) \leq x_k < \tau_k(i)\} \\
&= F_{w_k}(\tau_k(i-1) - h_k\theta) - F_{w_k}(\tau_k(i) - h_k\theta),
\end{aligned}
\tag{6}
$$

where $F_{w_k}(\cdot)$ denotes the CCDF of w_k. Clearly, for $i = 0$ (resp. $i = 2^{q(k)}$), the simplified expression $P(\boldsymbol{b}_k = \boldsymbol{v}(0); \theta) = 1 - F_{w_k}(\tau_k(1) - h_k\theta)$ (resp. $P(\boldsymbol{b}_k = \boldsymbol{v}(2^{q(k)}); \theta) = F_{w_k}(\tau_k(2^{q(k)} - 1) - h_k\theta)$) holds, given the "dummy" threshold $\tau_k(0) = -\infty$ (resp. $\tau_k(2^{q(k)}) = +\infty$) definition.

The problem here is the derivation of a (computationally) simple test (resorting to the decision statistic Λ) on the basis of $\{\boldsymbol{Y}, \boldsymbol{s}\}$ and the corresponding quantizer design for each dumb sensor. We highlight that the fusion rules and the (multi-bit) quantizer design obtained in this paper rely on the knowledge of the *noise* (through $\rho(\boldsymbol{b}_k = \boldsymbol{v}(j); \theta)$ and $P(\boldsymbol{b}_k = \boldsymbol{v}(j); \theta)$) and *channel models* (through $G_{q(k)}(P_{e,k}, d_{i,j})$), with optimization benefits reduced in the case of mismatch. Accordingly, the performance will be evaluated in terms of the well-known system detection $P_{D_0} \triangleq \Pr\{\Lambda > \gamma | \mathcal{H}_1\}$ and false-alarm probabilities $P_{F_0} \triangleq \Pr\{\Lambda > \gamma | \mathcal{H}_0\}$, where γ represents the usual system (decision) threshold, needed to ensure a desired false-alarm rate or to minimize the fusion error-probability [9].

III. FUSION RULES DESIGN

A common approach to handle detection in the presence of unknown parameters (viz. composite hypothesis testing) resorts to the GLRT [36]. For the DD problem at hand, the corresponding decision statistic is obtained by replacing the unknown parameter θ with its ML estimate $\hat{\theta}$ (under $\mathcal{H}_1$) in the LR, i.e. [26]

$$
\left\{ \Lambda_{\mathrm{G}} \triangleq \frac{p(\boldsymbol{Y}, \boldsymbol{s}; \hat{\theta})}{p(\boldsymbol{Y}, \boldsymbol{s}; \theta_0)} \right\} \underset{\mathcal{H}_0}{\overset{\mathcal{H}_1}{\gtrless}} \gamma,
\tag{7}
$$

where $\theta_0 = 0$, γ is the system threshold, and the ML estimate $\hat{\theta}$ is evaluated as

$$
\hat{\theta} \triangleq \arg\max_{\theta} p(\boldsymbol{Y}, \boldsymbol{s}; \theta).
\tag{8}
$$

It is clear from Eq. (7) that Λ_{G} requires the solution to an optimization problem, which *increases the computational burden* of its implementation.

For example, in the case of a WSN made of sole dumb sensors trying to reveal a signal buried in Gaussian noise, it

has been shown in [26] that $p(\boldsymbol{Y}, \boldsymbol{s}; \theta)$ is a concave function of θ, and consequently any one-dimensional gradient-based search starting from a random initial estimate is guaranteed to converge to the global maximum. Unfortunately, a closed form of $\hat{\theta}$ is not available even in this peculiar case.

Therefore, we resort to the Rao test a simpler and closed-form alternative to GLRT, available in closed-form for the broad class of unimodal noise PDFs. In this context, the Rao test is expressed in implicit form as [36]

$$
\left\{ \Lambda_{\mathrm{R}} \triangleq \frac{\left(\frac{\partial \ln p(\boldsymbol{Y}, \boldsymbol{s}; \theta)}{\partial \theta} \Big|_{\theta = \theta_0} \right)^2}{\mathrm{I}(\theta_0)} \right\} \underset{\mathcal{H}_0}{\overset{\mathcal{H}_1}{\gtrless}} \gamma,
\tag{9}
$$

where γ retains the same meaning as Eq. (7) and $\mathrm{I}(\theta_0)$ denotes the Fisher Information (FI), i.e. $\mathrm{I}(\theta) \triangleq \mathbb{E}\left\{ \left(\frac{\partial \ln[p(\boldsymbol{Y}, \boldsymbol{s}; \theta)]}{\partial \theta} \right)^2 \right\}$, evaluated at θ_0. The motivation of our choice is the extreme simplicity of the test implementation (since $\hat{\theta}$ is not required, cf. Eq. (9)), but with the same weak-signal asymptotic performance as the GLRT [36]. Hereinafter, we briefly describe the key steps needed to obtain the explicit form of Rao test.

First, the numerator term in Eq. (9) (before evaluation at $\theta = \theta_0$) can be expressed as shown in Eq. (11) at the top of next page (see Appendix A for a detailed proof), where $p'_{w_{K_q + \kappa}}(\cdot)$ represents the first derivative of $p_{w_{K_q + \kappa}}(\cdot)$ with respect to θ, and the auxiliary definition

$$
\begin{aligned}
\rho(\boldsymbol{b}_k = \boldsymbol{v}(i); \theta) &\triangleq \\
p_{w_k}(\tau_k(i-1) - h_k\theta) &- p_{w_k}(\tau_k(i) - h_k\theta),
\end{aligned}
\tag{10}
$$

has been employed.

Secondly, by denoting with $\mathrm{I}_q(\theta)$ and $\mathrm{I}_u(\theta)$ the FI corresponding to the set of dumb and smart sensors, respectively, it can be shown (the proof is given in Appendix B) that the total FI has the form reported in Eq. (12) at the top of next page, where the additional notation $\mathrm{I}_{w_{K_q + \kappa}} \triangleq \int [\partial \ln p_{w_{K_q + \kappa}}(\zeta)/\partial \zeta]^2 p_{w_{K_q + \kappa}}(\zeta) d\zeta$ has been exploited for compactness.

Thus, combining Eqs. (11) and (12), we obtain Λ_{R} in closed

$$\left(\frac{\partial \ln\left[p(\boldsymbol{Y}, \boldsymbol{s}; \theta)\right]}{\partial \theta}\right)^2 = \left(\sum_{k=1}^{K_q} \frac{h_k \sum_{i=1}^{2^{q(k)}} P(\boldsymbol{y}_k|\boldsymbol{b}_k = \boldsymbol{v}(i)) \rho(\boldsymbol{b}_k = \boldsymbol{v}(i); \theta)}{\sum_{i=1}^{2^{q(k)}} P(\boldsymbol{y}_k|\boldsymbol{b}_k = \boldsymbol{v}(i)) P(\boldsymbol{b}_k = \boldsymbol{v}(i); \theta)} - \sum_{\kappa=1}^{K_u} \frac{h_{K_q+\kappa} \, p'_{w_{K_q+\kappa}}\left(s_\kappa - h_{K_q+\kappa}\theta\right)}{p_{w_{K_q+\kappa}}\left(s_\kappa - h_{K_q+\kappa}\theta\right)}\right)^2 \quad (11)$$

$$\mathrm{I}(\theta) \triangleq \mathrm{I}_q(\theta) + \mathrm{I}_u(\theta) = \sum_{k=1}^{K_q} h_k^2 \sum_{i=1}^{2^{q(k)}} \frac{\left\{\sum_{j=1}^{2^{q(k)}} G_{q(k)}\left(P_{e,k}, d_{i,j}\right) \rho\left(\boldsymbol{b}_k = \boldsymbol{v}\left(j\right); \theta\right)\right\}^2}{\sum_{j=1}^{2^{q(k)}} G_{q(k)}\left(P_{e,k}, d_{i,j}\right) P\left(\boldsymbol{b}_k = \boldsymbol{v}\left(j\right); \theta\right)} + \sum_{\kappa=1}^{K_u} h_{K_q+\kappa}^2 \, \mathrm{I}_{w_{K_q+\kappa}} \quad (12)$$

---

form as

$$\Lambda_{\mathrm{R}} = \frac{1}{\mathrm{I}(\theta_0)} \left(\sum_{k=1}^{K_q} \frac{h_k \sum_{i=1}^{2^{q(k)}} P(\boldsymbol{y}_k|\boldsymbol{b}_k = \boldsymbol{v}(i)) \rho(\boldsymbol{b}_k = \boldsymbol{v}(i); \theta_0)}{\sum_{i=1}^{2^{q(k)}} P(\boldsymbol{y}_k|\boldsymbol{b}_k = \boldsymbol{v}(i)) P(\boldsymbol{b}_k = \boldsymbol{v}(i); \theta_0)}\right.$$
$$\left. - \sum_{\kappa=1}^{K_u} \frac{h_{K_q+\kappa} \, p'_{w_{K_q+\kappa}}\left(s_\kappa\right)}{p_{w_{K_q+\kappa}}\left(s_\kappa\right)}\right)^2 \quad (13)$$

Despite the seemingly difficulty in its evaluation, Λ_{R} can be easily evaluated as all the involved terms can be pre-computed off-line. Some relevant examples for calculation of the Rao auxiliary terms are reported in Tab. I for Gaussian, Laplace and Generalized Gaussian noise PDFs. Also, it is not difficult to show that the computational complexity involved is $\mathcal{O}\left(\sum_{k=1}^{K_q} 2^{q(k)} + K_u\right)$, i.e. with a linear scaling in the number of smart and dumb sensors, and an exponential scaling in the bit resolution.

Furthermore, it is apparent that Λ_{R} (as well as Λ_{G}) is a function of $\{\tau_k(i)\}_{i=0}^{2^{q(k)}}$, $k = 1, 2, \ldots, K_q$, through the terms $P(\boldsymbol{b}_k = \boldsymbol{v}(i); \theta_0)$ and $\rho(\boldsymbol{b}_k = \boldsymbol{v}(i); \theta_0)$ in the first sum of Eq. (13). Therefore, the thresholds of dumb sensors' (multi-bit) quantizers can be optimized to achieve improved performance. More specifically, one of the objectives of this work is to design quantizers which are *asymptotically-optimal* (the meaning will be clarified in what follows). Next section is devoted to fulfill this objective.

IV. QUANTIZER DESIGN FOR DUMB SENSORS

In this section, we first state results for the asymptotic performance of the GLRT and the Rao test. Then, we focus on asymptotically-optimal quantizer design for dumb sensors. According to [36], the asymptotic (i.e. large WSN) PDF of Λ_{R} (as well as $2\ln\Lambda_{\mathrm{G}}$) is[3]

$$\Lambda_{\mathrm{R}} \overset{a}{\sim} \begin{cases} \chi_1^2 & \text{under} \quad \mathcal{H}_0 \\ \chi_1'^2(\lambda_{q+u}) & \text{under} \quad \mathcal{H}_1 \end{cases} \quad (14)$$

where the non-centrality parameter λ_{q+u} (the subscript $(\cdot)_{q+u}$ is employed here to underline that both dumb and smart

[3]We notice that Eq. (14) holds for $\mathcal{H}_1$ under the weak-signal condition, i.e., θ is assumed to be relatively small compared to the noise variance [36]. Indeed, for most WSN applications, weak-signal detection is of primary interest. On the other hand, if the signal to be detected is strong, a few sensors adopting naive quantization schemes (e.g., a uniform quantizer) would suffice.

sensors contribute to the non-centrality parameter) is given by

$$\lambda_{q+u} \triangleq (\theta_1 - \theta_0)^2 \, \mathrm{I}(\theta_0) = \theta_1^2 \, \mathrm{I}(\theta_0), \quad (15)$$

with θ_1 being the true value under $\mathcal{H}_1$ (in our case $\theta_0 = 0$). Clearly the larger λ_{q+u}, the better the GLRT and Rao tests will perform.

From Eq. (15) we can see that the non-centrality parameter λ_{q+u} is a *monotonically increasing* function of the FI evaluated at $\theta = 0$. The latter is a function of the $\left(2^{q(k)} - 1\right)$-dimensional quantization threshold vectors $\boldsymbol{\tau}_k \triangleq \left[\tau_k(1), \ldots, \tau_k(2^{q(k)} - 1)\right]$, where the two extreme thresholds are obviously fixed as $\tau_k(0) = -\infty$ and $\tau_k(2^{q(k)}) = +\infty$. In other words, by optimally choosing the quantizer thresholds $\boldsymbol{\tau}_k$'s for dumb sensors, we can *optimize* the detection performance of the Rao test (viz. GLRT).

As a consequence, the asymptotic detection performance of the Rao test (as well as GLRT) can be optimized by solving the following optimization problem

$$\max_{\{\boldsymbol{\tau}_k\}_{k=1}^{K_q}} \mathrm{I}_q\left(\theta_0, \{\boldsymbol{\tau}_k\}_{k=1}^{K_q}\right), \quad (16)$$

where (a) the term $\mathrm{I}_u(\theta_0) = \mathrm{I}_u$ is not included since it is *independent* from the quantization thresholds and (b) we have highlighted, with a slight abuse of notation, the dependence of the FI on the $\boldsymbol{\tau}_k$'s.

Finally, exploiting mutual independence of distortion channels, the optimization problem can be further decoupled (see Eq. (12)) into the following K_q independent optimization problems

$$\boldsymbol{\tau}_k^\star \triangleq \arg\max_{\boldsymbol{\tau}_k} g_k(\boldsymbol{\tau}_k), \quad k = 1, \ldots, K_q, \quad (17)$$

where the explicit form of $g_k(\boldsymbol{\tau}_k)$ is given as follows:

$$g_k(\boldsymbol{\tau}_k) \triangleq \sum_{i=1}^{2^{q(k)}} \frac{\left\{\sum_{j=1}^{2^{q(k)}} G_{q(k)}\left(P_{e,k}, d_{i,j}\right) \rho\left(\boldsymbol{b}_k = \boldsymbol{v}(j); \theta_0\right)\right\}^2}{\sum_{j=1}^{2^{q(k)}} G_{q(k)}\left(P_{e,k}, d_{i,j}\right) P\left(\boldsymbol{b}_k = \boldsymbol{v}(j); \theta_0\right)}. \quad (18)$$

We remark that each problem is subject to the ordered constraints $\tau_k(i) < \tau_k(i+1)$, for $i = 1, \ldots 2^{q(k)} - 1$.

Remark: It is worth noticing that in the ideal BSC case ($P_{e,k} = 0$), the objective $g_k(\boldsymbol{\tau}_k)$ assumes the following

w_k	$P(\boldsymbol{b}_k = \boldsymbol{v}(i); \theta_0)$	$\rho(\boldsymbol{b}_k = \boldsymbol{v}(i); \theta_0)$
$\sim \mathcal{N}(0, \sigma_w^2)$ **(Gaussian)**	$\mathcal{Q}\left(\frac{\tau_k(i-1)}{\sigma_w}\right) - \mathcal{Q}\left(\frac{\tau_k(i)}{\sigma_w}\right)$	$\frac{1}{(2\pi\sigma_w^2)^{1/2}}\left[\exp\left(-\frac{\tau_k(i-1)^2}{2\sigma_w^2}\right)\right.$ $\left. - \exp\left(-\frac{\tau_k(i)^2}{2\sigma_w^2}\right)\right]$
$\sim \mathcal{L}(0, \beta)$ **(Laplace)**	$\frac{1}{2}\left\{\text{sign}[\tau_k(i)]\left[1 - \exp\left(\frac{\|\tau(i)\|}{\alpha}\right)\right]\right.$ $\left. -\text{sign}[\tau_k(i-1)]\left[1 - \exp\left(\frac{\|\tau(i-1)\|}{\alpha}\right)\right]\right\}$	$\frac{1}{2\beta}\left[\exp\left(-\frac{\|\tau_k(i-1)\|}{\beta}\right)\right.$ $\left. - \exp\left(-\frac{\|\tau_k(i)\|}{\beta}\right)\right]$
$\sim \mathcal{GN}(0, \alpha, \epsilon)$ **(Gen. Gaussian)**	$\frac{1}{2\Gamma(1/\epsilon)}\left\{\text{sign}[\tau_k(i)]\,\gamma\left[\frac{1}{\epsilon}, \left(\frac{\|\tau(i)\|}{\alpha}\right)^\epsilon\right]\right.$ $\left. -\text{sign}[\tau_k(i-1)]\,\gamma\left[\frac{1}{\epsilon}, \left(\frac{\|\tau(i-1)\|}{\alpha}\right)^\epsilon\right]\right\}$	$\frac{\epsilon}{2\alpha\Gamma(1/\epsilon)}\left[\exp\left(-\left[\frac{\|\tau_k(i-1)\|}{\alpha}\right]^\epsilon\right)\right.$ $\left. - \exp\left(-\left[\frac{\|\tau_k(i)\|}{\alpha}\right]^\epsilon\right)\right]$

TABLE I: Auxiliary terms needed for Rao test computation evaluated for some noteworthy noise PDFs.

simplified expression (since $G_{q(k)}(P_{e,k}, d_{i,j}) = 1$ only if $i = j$):

$$g_k(\boldsymbol{\tau}_k) \triangleq \sum_{i=1}^{2^{q(k)}} \frac{\rho(\boldsymbol{b}_k = \boldsymbol{v}(i); \theta_0)^2}{P(\boldsymbol{b}_k = \boldsymbol{v}(i); \theta_0)} \quad (19)$$

Additionally, as explained in Sec. II, we stress out that the proposed optimization relies on the perfect knowledge of the *noise* (through $\rho(\boldsymbol{b}_k = \boldsymbol{v}(j); \theta)$ and $P(\boldsymbol{b}_k = \boldsymbol{v}(j); \theta)$) and *channel models* (through $G_{q(k)}(P_{e,k}, d_{i,j})$).

Clearly, given the same asymptotic performance achieved by both GLRT and Rao test, the optimization problem (17) has the same form as [26, Eq. (22)], developed to optimize the performance of the more complex GLRT. Consequently, we can utilize the same method there, i.e. the PSOA, to search the optimal quantization thresholds in Eq. (17).

In brief, the PSOA is an iterative stochastic optimization approach[4] inspired by the social cooperative and competitive behaviors of bird flocking and fish schooling, resorting to a swarm of $m = 1, \ldots, M$ particles to tackle high-dimensional, non-convex optimization problems [38]. Accordingly, the objective and the vector argument will be referred to as $g(\cdot)$ and $\boldsymbol{\tau}$ (as opposed to $g_k(\cdot)$ and $\boldsymbol{\tau}_k$, respectively).

When applying the PSOA to Eq. (17), we assume that a swarm of M particles is employed to explore the $(2^q - 1)$-dimensional space $\boldsymbol{\Delta}$ in search of a (hopefully) globally-optimal solution. Also, we assume that the search interval for each dimension is restricted to $[-\tau_{\max}, \tau_{\max}]$, where $\tau_{\max}$ denotes the maximum position limitation (see [26] for a detailed explanation), that is $\boldsymbol{\Delta} \triangleq [-\tau_{\max}, \tau_{\max}]^{2^q-1}$.

At the ℓth iteration, the mth particle is described by two characteristics: the position $\boldsymbol{\tau}_m^\ell = [\tau_m^\ell(1), \tau_m^\ell(2), \ldots, \tau_m^\ell(2^q - 1)]$ (representing the argument of the objective) and the velocity $\boldsymbol{\nu}_m^\ell = [\nu_m^\ell(1), \nu_m^\ell(2), \ldots, \nu_m^\ell(2^q-1)]$ (corresponding to the direction of improvement) vectors. The PSOA evolution is characterized by the best personal position of mth particle $\boldsymbol{pbest}_m^\ell$ (i.e. the argument of the objective which achieved the highest value so far) and the overall best position denoted with $\boldsymbol{sbest}^\ell$ (representing its collective behaviour). The (iterative) PSOA is summarized as **Algorithm 1** and detailed henceforth.

Init: At the init step ($\ell = 0$), for mth particle position we first randomly (and independently) initialize $\tau_m^0(n) \sim \mathcal{U}(-\tau_{\max}, \tau_{\max})$ for $n = 1, \ldots, 2^q - 1$, and then sort them

in *ascending order*. Additionally, in order to prevent the particles from leaving the search space $\boldsymbol{\Delta}$, we initialize $\boldsymbol{\nu}_m^0$ according to a uniform distribution in $[-\nu_{\max}, \nu_{\max}]$, where $\nu_{\max} = [\tau_{\max} - (-\tau_{\max})]/2 = \tau_{\max}$, following [38].

Based on the initial particles positions $\{\boldsymbol{\tau}_m^0\}_{m=1}^M$, we set the initial personal best position $\boldsymbol{pbest}_m^0$ of the mth particle to be

$$\boldsymbol{pbest}_m^0 = \boldsymbol{\tau}_m^0, \ m = 1, 2, \ldots, M. \quad (20)$$

Substituting the initial particles $\{\boldsymbol{\tau}_m^0\}_{m=1}^M$ into the objective function $g(\cdot)$ in (18), we obtain a set of values $\{g(\boldsymbol{\tau}_m^0)\}_{m=1}^M$, which allow to set the initial global best position $\boldsymbol{sbest}^0$ as

$$\boldsymbol{sbest}^0 = \arg\max_{\{\boldsymbol{\tau}_m^0\}_{m=1}^M}\{g(\boldsymbol{\tau}_1^0), g(\boldsymbol{\tau}_2^0), \ldots, g(\boldsymbol{\tau}_M^0)\}. \quad (21)$$

Update: At the $(\ell + 1)$th iteration, the position $(\boldsymbol{\tau}_m^{\ell+1})$ and velocity $(\boldsymbol{\nu}_m^{\ell+1})$ vectors of mth particle are updated as:

$$\begin{cases} \boldsymbol{\tau}_m^{\ell+1} \triangleq \boldsymbol{\tau}_m^\ell + \boldsymbol{\nu}_m^{\ell+1}, \\ \boldsymbol{\nu}_m^{\ell+1} \triangleq \text{cf} \cdot [\boldsymbol{\nu}_m^\ell + c_1\, r_{m,1}^\ell\, (\boldsymbol{pbest}_m^\ell - \boldsymbol{\tau}_m^\ell) \\ \qquad\qquad + c_2\, r_{m,2}^\ell\, (\boldsymbol{sbest}^\ell - \boldsymbol{\tau}_m^\ell)], \end{cases} \quad (22)$$

where $r_{m,1}^\ell$ and $r_{m,2}^\ell$ are randomly drawn such that $r_{m,j}^\ell \sim \mathcal{U}(0,1)$; the positive (tunable) constants c_1 and c_2 represent the acceleration coefficients that "attract" the particles towards the personal best and global positions, respectively; κ is a *constriction factor* evaluated as $\text{cf} \triangleq 2\,/\,|2 - \varphi - \sqrt{\varphi^2 - 4\varphi}|$, where $\varphi \triangleq c_1 + c_2$ (the coefficients c_j are chosen to ensure $\varphi > 4$). For the order constraint in (17), we sort the elements of $\tau_m(n)$ (given m) in *ascending* order for $n = 1, \ldots, 2^q - 1$. Notice that it is possible for some particles to move outside $[-\tau_{\max}, \tau_{\max}]^{2^q-1}$ during the iteration process. To avoid this, we impose the following *correction step* at each iteration (immediately after Eq. (22) and ordering operation):

$$\begin{cases} \tau_m^{\ell+1}(n) \to \tau_{\max}; & \text{if} \quad \tau_m^{\ell+1}(n) > \tau_{\max} \\ \tau_m^{\ell+1}(n) \to -\tau_{\max}; & \text{if} \quad \tau_m^{\ell+1}(n) < -\tau_{\max} \\ \tau_m^{\ell+1}(n) \to \tau_m^{\ell+1}(n); & \text{otherwise} \end{cases} \quad (23)$$

The update criterion for the best personal position of mth particle at $(\ell + 1)$ iteration is (straightforwardly) given by

$$\boldsymbol{pbest}_m^{\ell+1} \triangleq \begin{cases} \boldsymbol{pbest}_m^\ell & \text{if } g(\boldsymbol{\tau}_m^{\ell+1}) \leq g(\boldsymbol{pbest}_m^\ell) \\ \boldsymbol{\tau}_m^{\ell+1} & \text{if } g(\boldsymbol{\tau}_m^{\ell+1}) > g(\boldsymbol{pbest}_m^\ell) \end{cases} \quad (24)$$

---

[4]In the following, for the sake of a lighter notation, we will drop the subscript "k" referring to the sensor index, so as to generically focus on the optimization of a generic (dumb) sensor.

Accordingly, the global best position at $(\ell + 1)$th iteration $\boldsymbol{sbest}^{\ell+1}$ is obtained by comparing all the personal best positions at the same iteration, namely

$$\boldsymbol{sbest}^{\ell+1} \triangleq \underset{\{\boldsymbol{pbest}_m^{\ell+1}\}_{m=1}^M}{\arg\max} \{g(\boldsymbol{pbest}_1^{\ell+1}), \dots, g(\boldsymbol{pbest}_M^{\ell+1})\} \tag{25}$$

Termination: The update step is repeated until the following *exit condition* is met

$$\max_{m=1,\dots,M} \|\boldsymbol{\nu}_m^\ell\| \leq \nu_{tol}, \tag{26}$$

where ν_{tol} denotes the stop tolerance velocity.

Algorithm 1 : PSOA for Quantizer Optimization [26].

Input: q, M, $\tau_{\max}$, c_j, ν_{tol};
Output: a solution $\boldsymbol{\tau}^\star$ for each optimization problem in Eq. (17).
 1: Set $\ell = 0$;
 2: **for** $m = 1, \dots, M$ **do**
 3:     randomly initialize $\boldsymbol{\tau}_m^0 \in [-\tau_{\max}, \tau_{\max}]^{2^q-1}$ and $\boldsymbol{\nu}_m^0 \in [-\tau_{\max}, \tau_{\max}]^{2^q-1}$;
 4:     Alter the initial position $\boldsymbol{\tau}_m^0$ by sorting ascendingly its entries;
 5:     Evaluate $g(\boldsymbol{\tau}_m^0)$ and set $\boldsymbol{pbest}_m^0$ via Eq. (20);
 6: **end for**
 7: Set $\boldsymbol{sbest}^0$ via Eq. (21);
 8: **do**
 9:     **for** $m = 1, \dots, M$ **do**
10:         Update the velocity $\boldsymbol{\nu}_m^{\ell+1}$ and the position $\boldsymbol{\tau}_m^{\ell+1}$ via Eq. (22);
11:         Alter the position $\boldsymbol{\tau}_m^{\ell+1}$ by sorting ascendingly its entries and correction step in Eq. (23);
12:         Evaluate $g(\boldsymbol{\tau}_m^{\ell+1})$ and update $\boldsymbol{pbest}_m^{\ell+1}$ via Eq. (24);
13:     **end for**
14:     Update $\boldsymbol{sbest}^{\ell+1}$ according to Eq. (25);
15:     Set $\ell \to \ell + 1$;
16: **until** $\max_{m=1,\dots,M} \|\boldsymbol{\nu}_m^{\ell+1}\| \leq \nu_{tol}$;
17: $\boldsymbol{\tau}^\star = \boldsymbol{sbest}^{\ell+1}$.

V. ASYMPTOTIC DETECTION GAINS

Tackling a complementary analysis to [34] (referring to a decentralized estimation problem), we now establish the detection gain provided by the use of dumb sensors, employing *arbitrarily multi-level quantized* (i.e. non-necessarily designed according to the criterion devised in Sec. IV) measurements. To this end, by relying on Eq. (14), we express the asymptotic detection probability P_{D_0} as a function of the asymptotic probability of false-alarm P_{F_0}:

$$P_{D_0}(\lambda_{(q\to s)+u}, P_{F_0}) = \mathcal{Q}\left(\mathcal{Q}^{-1}(P_{F_0}/2) - \sqrt{\lambda_{(q\to s)+u}}\right) + \mathcal{Q}\left(\mathcal{Q}^{-1}(P_{F_0}/2) + \sqrt{\lambda_{(q\to s)+u}}\right), \tag{27}$$

where the subscript "$(q \to s) + u$" indicates the adoption of dumb sensors with s-bit resolution for the multi-level quantizer, along with smart sensors. Apparently, $q \to 0$

denotes the absence of dumb sensors in the WSN, and it is equivalent to $P_{D_0}(\lambda_u, P_{F_0})$, i.e. the (asymptotic) detection probability achieved with the *sole use* of smart sensors. Also, for DD problem under consideration, it holds the simpler form $\lambda_{(q\to s)+u} = \lambda_{(q\to s)} + \lambda_u$, i.e. the non-centrality parameter can be expressed as the sum of the contributions of dumb and smart sensors, respectively. Finally, we recall that the above asymptotic P_{D_0} expression relies on the same assumptions required for the quantizer design in Sec. IV, i.e. knowledge of both (sensing) noise and (communication) channel statistics.

Based on these explicit quantities, we are able to define the *Asymptotic Detection Gain* (ADG) between a WSN employing s-bit resolution and one employing t-bit resolution ($t > s$) as

$$G_d(P_{F_0}) \triangleq P_{D_0}(\lambda_{(q\to t)+u}, P_{F_0}) - P_{D_0}(\lambda_{(q\to s)+u}, P_{F_0}), \tag{28}$$

to measure the increase in detection rate arising from the use of finer quantizers. Additionally, we define the *Asymptotic Normalized Detection Gain* (ANDG) as

$$\bar{G}_d(P_{F_0}) \triangleq \frac{P_{D_0}(\lambda_{(q\to t)+u}, P_{F_0}) - P_{D_0}(\lambda_{(q\to s)+u}, P_{F_0})}{P_{D_0}(\lambda_{(q\to t)+u}, P_{F_0})}, \tag{29}$$

to assess the corresponding relative increment. It is worth noticing that both these measures can be employed to quantify:

1) the (normalized) detection gain when using dumb sensors other than smart sensors (following [34]), i.e. $q \to 0$ and $\lambda_{(q\to s)+u} = \lambda_u$;
2) the (normalized) detection gain when increasing the bit resolution from $s > 0$ to t bits.

Qualitative profiles of ADG and ANDG in the above relevant cases will be analyzed and commented later in Sec. VI.

VI. NUMERICAL RESULTS

In this section, we perform and investigate threshold optimization via PSOA (Sec. IV) for both Rao test and GLRT, compare their relative performance, and also assess the impact of improvements in quantization resolution on the (asymptotic) detection capabilities of the detectors, resorting to the asymptotic detection gains defined in Sec. V.

Herein, we define the kth sensor observation Signal-to-Noise Ratio (SNR) as $\Gamma_k \triangleq (h_k^2\theta^2/\mathbb{E}\{w_k^2\})$. For simplicity, in what follows we assume $h_k = h$ and $p_{w_k}(\cdot) = p_w(\cdot)$ for all the sensors, and $P_{e,k} = P_e$ for all dumb sensors. These parameters determine a (simplified) homogeneous scenario, e.g. $\Gamma_k = \Gamma$, $k = 1, \dots K$. In addition, without loss of generality, we set $h = 1$ and $\mathbb{E}\{w_k^2\} = 1$, respectively.

A. PSOA for Threshold Set Choice

We first analyze the result of PSOA in optimizing the function $g(\boldsymbol{\tau})$ (cf. Eq. (18)) with respect to the vector of quantization thresholds $\boldsymbol{\tau}$. Indeed recall that, since we are considering a homogeneous scenario, the optimization function is the same for all the sensors, i.e. $g_k(\cdot) = g(\cdot)$, $k = 1, \dots, K$.

To investigate in detail PSOA capabilities in optimizing different noise PDFs, we investigate *two* relevant scenarios. Specifically, we consider threshold set design in the cases

of (i) Gaussian noise, that is $p_w(\omega) = \frac{1}{(2\pi\sigma_w^2)^{\frac{1}{2}}} \exp(-\frac{\omega^2}{2\sigma_w^2})$ and (ii) Generalized Gaussian noise, that is $p_w(\omega) = \frac{\epsilon}{2\alpha\Gamma(1/\epsilon)} \exp\left[-(\frac{|\omega|}{\alpha})^\epsilon\right]$, respectively. We observe that scenario (i) corresponds to a widely-employed noise PDF arising due to many independent contributions (as a result of the central limit theorem), while scenario (ii) represents a flexible class of PDFs allowing to model long-tail behaviour, e.g. possibly due to outliers. It is known from [22] that $\tau^* = 0$ holds for $q = 1$ in cases of Gaussian and Generalized Gaussian (only when $0 < \epsilon \le 2$) distributions. On the other hand, when $\epsilon > 2$, $g(\tau)$ becomes bimodal and $\tau^* \ne 0$. For the mentioned reasons, to stress PSOA capabilities and diversify our analysis, we will consider $\epsilon = 3$ in the GGD case.

Furthermore, to appreciate adaptiveness to different reporting channel conditions, we will consider both *ideal* and *imperfect* channel scenarios, i.e. $P_e \in \{0, 0.2\}$. Finally, referring to PSOA parameters, we set $M = 300$, $\tau_{\max} = 5$, $c_1 = c_2 = 2.05$ and $\nu_{tol} = 10^{-6}$, respectively.

Accordingly, in Figs. 2(a) and 2(b), we show the position of the optimized thresholds for an increasing bit resolution, i.e. $q \in \{1, 2, 3\}$, respectively, for $w_k \sim \mathcal{N}(0, \sigma_w^2)$ and $\mathcal{GN}(0, \alpha, 3)$, respectively. From inspection of the results, it can be seen that in the case of Gaussian noise, the optimized threshold $\tau^\star$ is *zero* for $q = 1$ and the displacement of the threshold set $\boldsymbol{\tau}^\star$ *symmetric* for $q \in \{2, 3\}$. This is consistent with the results in [19], [22] and [26], respectively. On the other hand, in GGD case, the optimized threshold $\tau^\star$ is *non-zero* for $q = 1$ (as observed in [22], [28]), and the displacement of the threshold set $\boldsymbol{\tau}^\star$ becomes *asymmetric* for $q \in \{2, 3\}$. Additionally, by analyzing the two different reporting channel conditions, an imperfect BSC ($P_e = 0.2$) does not affect symmetry (although makes the quantization intervals more irregular) in the Gaussian case (thus agreeing with [26]), whereas the same non-ideal channel conditions partially-mitigate the asymmetry of $\tau^\star$ in GGD case. The latter effect was observed, for the simple case $q = 1$, in [22], [28].

B. Rao Test Versus GLRT

We now turn our attention to performance comparison of *threshold-optimized* Rao test and GLRT in a WSN with a finite number of sensors (since, *asymptotically*, they share the same performance [36]). For the mentioned reason, we consider a WSN with $K_q = 5$ dumb sensors using $q = 1, 2, 3$ quantization bits and $K_u = 2$ smart sensors. Herein, we assume $\theta = 1$, which implies $\Gamma = 0\,\mathrm{dB}$. We remark that lower SNR values imply a condition in which the GLRT and Rao test would lead approximately to the same performance, due to the low-signal design assumption underlying Rao score test [36].

For the sake of completeness, corresponding WSNs with $(K_q + K_u) = 7$ and $K_u = 2$ smart sensors are assumed as a reference, providing an *upper and lower bounds* on the performance, respectively. It is worth noticing that in Gaussian case, GLR and Rao statistics coincide in the unquantized (viz.
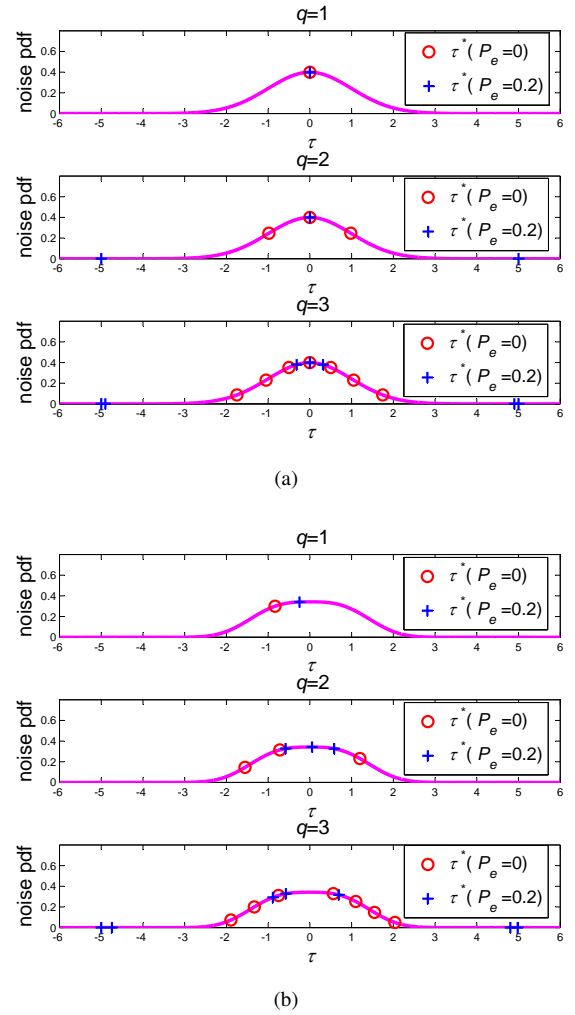

(a)

(b)

Fig. 2: Quantizer thresholds obtained by PSOA for a varying number of bits $q = 1, 2, 3$ with $P_e = 0, 0.2$ under (a): Gaussian and (b): Generalized Gaussian ($\epsilon = 3$) noise background, respectively.

only smart-sensor) case, and are given in closed form as

$$\Lambda^{\mathrm{upp}} = \left(\sum_{k=1}^{K} \frac{h_k s_k}{\sigma_{w,k}^2}\right)^2 \Big/ \left(\sum_{k=1}^{K} \frac{h_k^2}{\sigma_{w,k}^2}\right) \quad (30)$$

On the other hand, in GGD case their expressions differ. Specifically, the GLR statistic in the unquantized case is equal to

$$\Lambda_{\mathrm{G}}^{\mathrm{upp}} = \left(\sum_{k=1}^{K} \frac{|s_k - h_k\hat{\theta}|}{\alpha_{w,k}}\right)^{\epsilon_k} \Big/ \left(\sum_{k=1}^{K} \frac{|s_k|}{\alpha_{w,k}}\right)^{\epsilon_k} \quad (31)$$

whereas the Rao statistic closed-form is

$$\Lambda_{\mathrm{R}}^{\mathrm{upp}} = \frac{\left(\sum_{k=1}^{K} h_k \frac{\epsilon_k \operatorname{sign}(s_k)|s_k|^{(\epsilon_k-1)}}{\alpha_k^{\epsilon_k}}\right)^2}{\sum_{k=1}^{K} h_k^2 \frac{\epsilon_k(\epsilon_k-1)\Gamma(1-1/\epsilon_k)}{\alpha_k^2 \Gamma(1/\epsilon_k)}} \quad (32)$$

Then, in Fig. 3 we illustrate P_{D_0} vs. P_{F_0} (viz. Receiver Operating Characteristic, ROC) in a WSN with $w_k \sim \mathcal{N}\left(0, \sigma_w^2\right)$, whereas in Fig. 4 we illustrate analogous results pertaining to

a WSN with $w_k \sim \mathcal{GN}(0, \alpha, 3)$. In both figures, we report the results for the two BEP levels $P_e \in \{0, 0.2\}$. All the results are based on 10^5 Monte Carlo runs.

First, it is shown that the proposed Rao test (as well as the GLRT) works well in the presence of a hybrid combination of both dumb and smart sensors. Secondly, it is apparent that the ROC performance of the GLR and Rao tests are practically the same for Gaussian noise scenario. On the other hand, in GGD case, the performance of GLRT and Rao test in the finite sensor case slightly differs. This is reasonable both for unquantized measurements (since the expressions in Eqs. (31) and (32) are different), and for quantized measurements (since, in general, the performance of GLRT and Rao test may differ in the finite sensor case). Nonetheless, the implementation of the Rao test has the advantage of being significantly simpler than the GLRT (linear with the number of sensors). Finally, the implementation of multi-bit quantization shows a significantly higher detection probability than one-bit quantization in both noise scenarios considered. In particular, the detection performance of the hybrid combination (smart + 3-bit quantized sensors) is very close to the upper-bound, when the channel is perfect. On the other hand, in the presence of reporting channel errors (e.g., $P_e = 0.2$ in this example), the WSN performance degrades and the whole system is limited by the uncertainty of the communication channel.

As a complementary analysis, in Figs. 5 and 6 to assess the sensitivity of the considered threshold-optimized rules to the uncertainty in the knowledge of (i) reporting channel error and (ii) noise statistics, we focus on the case $q = 3$, $P_e = 0.1$ and $\Gamma = 0 \, \text{dB}$. In the *first* analysis, we assume that Rao test and GLRT have been derived (and optimized) both in *matched* (i.e. $\hat{P}_e = 0.1$) and *mismatched* scenarios (i.e. $\hat{P}_e = 0.2$) with respect to the channel error probability. Similarly, in the *second* analysis, we assume that Rao test and GLRT have been derived (and optimized) both in *matched* (i.e. $\Gamma = 0 \, \text{dB}$) and *mismatched* scenarios (i.e. $\Gamma = 3 \, \text{dB}$) with respect to the SNR value. As apparent from both figures, although there is a slight degradation in both the mismatched cases, the performance loss is not significant, thus proving some robustness of the proposed design. Clearly, higher uncertainty in the noise and/or channel error statistics would require implicit estimation of these parameters, based on adaptive designs.

C. Asymptotic Detection Gains

Finally, we investigate the asymptotic trends of WSN detection capabilities by means of the ADG and the ANDG defined in Sec. V (Eqs. (28) and (29), respectively). We recall that, since these are defined based on the asymptotic performance of GLRT and Rao test, *they apply to both* and are thus independent on the peculiar fusion rule considered at the FC. In the following analysis, we take into account the presence of both smart and dumb sensors to assess explicitly the detection gain (i) from using dumb sensors other than smart sensors and (ii) from increasing the bit resolution of dumb sensors, respectively. Henceforth, dumb sensors' quantizers are *threshold-optimized* according to the criterion
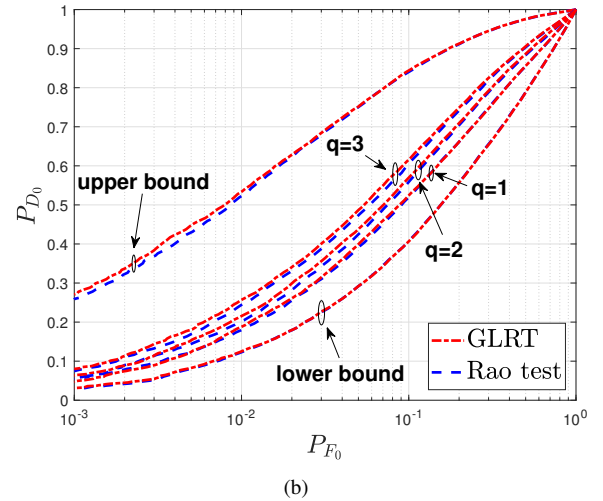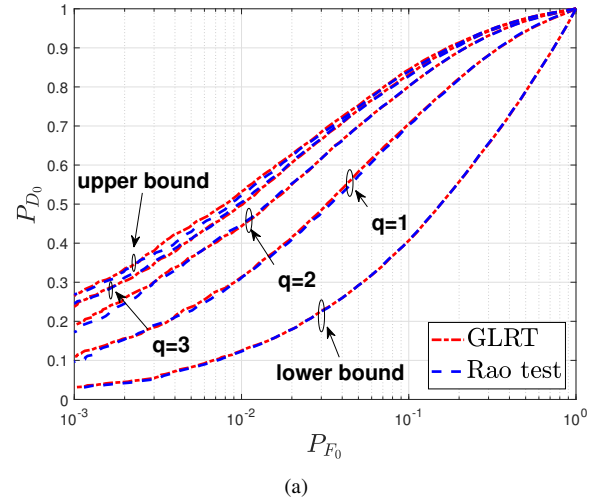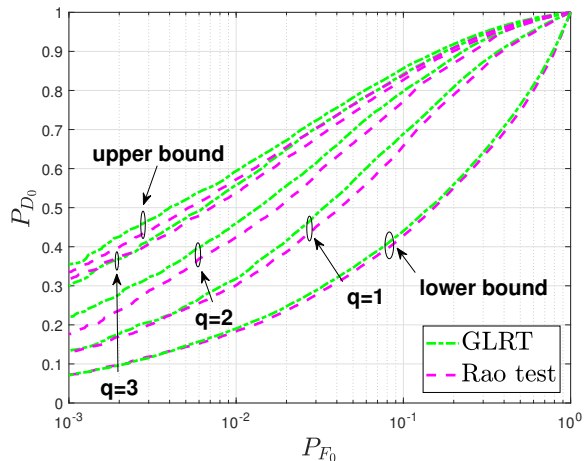

Fig. 3: P_{D_0} vs P_{F_0}; WSN for Gaussian noise $w_k \sim \mathcal{N}\left(0, \sigma^2\right)$ with (a): $P_e = 0$; (b): $P_e = 0.2$.

in Sec. IV. Nonetheless, as remarked in Sec. IV, the provided ADG/ANDG formulas *apply to any multi-bit quantizer choice*, e.g. also to uniform quantization.

To this end, in Figs. 7.(a) and 7.(b) we draw the aforementioned ADG (viz. $G_d(P_{F_0})$) and ANDG (viz. $\bar{G}_d(P_{F_0})$), respectively, in a WSN with $K_q = 5$, $K_u = 2$ and Gaussian noise, e.g. $w_k \sim \mathcal{N}\left(0, \sigma_w^2\right)$. Similarly, in Figs. 8.(a) and 8.(b) we illustrate the same metrics in a WSN with Generalized Gaussian noise, e.g. $w_k \sim \mathcal{GN}(0, \alpha, 3)$. The two noise scenarios are considered in conjunction with the channel cases $P_e \in \{0, 0.2\}$. Finally, we will consider *three* (s, t) configurations: *one* corresponding to the addition of (one-bit) dumb sensors to a WSN with ($K_u = 2$) smart sensors (i.e. $(s, t) = (0, 1)$) and *two* corresponding from a resolution increase of dumb sensors (i.e. $(s, t) = (1, 2)$ and $(s, t) = (1, 3)$, respectively).

First, it is apparent a different behavior for $G_d(P_{F_0})$ (unimodal) and $\bar{G}_d(P_{F_0})$ (decreasing), respectively. This is explained as any gain from resolution increase (or dumb sensors' addition) has its effect decreased (increased) on $G_d(P_{F_0})$ as P_{F_0} tends to one (resp. to zero), since accordingly, also P_{D_0}

(a)
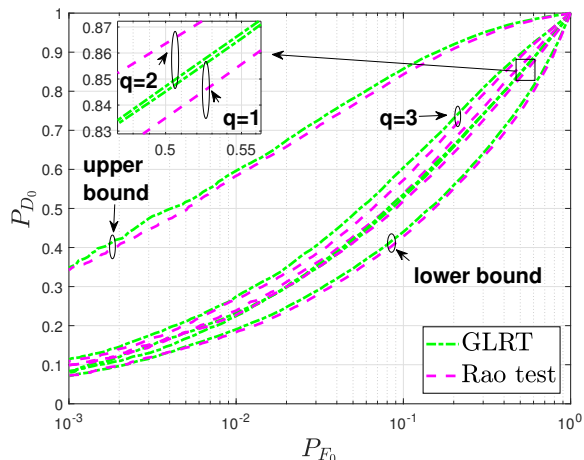
(b)

Fig. 4: P_{D_0} vs P_{F_0}; WSN for Generalized Gaussian noise $w_k \sim \mathcal{GN}(0, \alpha, 3)$ with (a): $P_e = 0$; (b): $P_e = 0.2$.
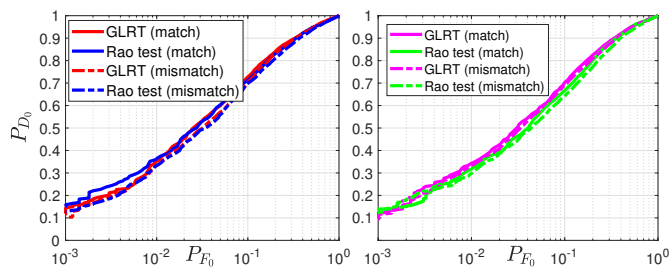

Fig. 5: P_{D_0} vs P_{F_0}; WSN for Gaussian noise $w_k \sim \mathcal{N}(0, \sigma^2)$ (left) and Generalized Gaussian noise $w_k \sim \mathcal{GN}(0, \alpha, 3)$ (right) with $q = 3$, $P_e = 0.1$ and $\hat{P}_e = 0.1$ (resp. $\hat{P}_e = 0.2$) in the matched (resp. mismatched) case.
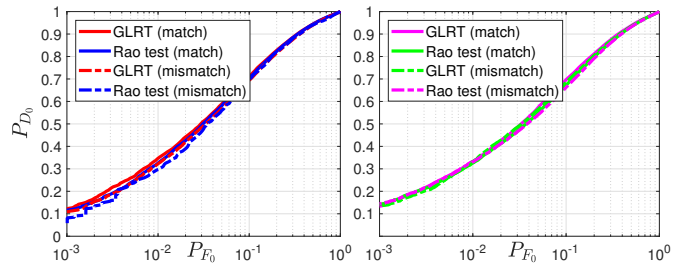

Fig. 6: P_{D_0} vs P_{F_0}; WSN for Gaussian noise $w_k \sim \mathcal{N}(0, \sigma^2)$ (left) and Generalized Gaussian noise $w_k \sim \mathcal{GN}(0, \alpha, 3)$ (right) with $q = 3$, $\Gamma = 0\,\mathrm{dB}$ and $\widehat{\Gamma} = 0\,\mathrm{dB}$ (resp. $\widehat{\Gamma} = 3\,\mathrm{dB}$) in the matched (resp. mismatched) case.

will tend to unity (resp. to zero), independently on the WSN considered. On the other hand, in $\bar{G}_d(P_{F_0})$, the trend for P_{F_0} in proximity of zero is suppressed by the normalization in Eq. (29). Secondly, the figures reveal that a configuration with *both* dumb and smart sensors can significantly improve system performance against one with *only* smart sensors, at the expenses of modestly-increased bandwidth requirements. Thirdly, compared to one-bit quantization, the implementation of multi-bit quantization can further improve detection performance. However, a less appreciable gain is observed when considering three-bit quantizers as opposed to two-bit ones. Finally, we observe that a degraded channel reasonably affects in a negative fashion both ADG/ANDG in $(s, t) = (0, 1)$ configuration, because of the less informative bits received from dumb sensors. On the other hand, in the other two configurations the relative trend of ADG/ANDG with respect to their ideal-channel counterparts is less intuitive and depends on both the configuration and the type of noise considered.

VII. CONCLUSIONS AND FURTHER DIRECTIONS

We proposed the Rao test for DD of an unknown deterministic signal in WSNs in zero-mean, unimodal and symmetric noise. The WSN model considered is quite general, as it encompasses both smart sensors (i.e. reporting full-precision measurements to the FC) and dumb sensors (employing multi-bit quantization and transmitting these bits over non-ideal and non-identical BSCs). The Rao fusion rule proposed represents a *simpler* (and thus attractive) *alternative* to GLRT, since it is in closed form (even under such general model) and obviates the need for cumbersome ML estimation. Additionally, we provided the explicit expression of the asymptotic (weak-signal) performance of Rao (viz. GLRT) fusion rule, here exploited from a *two-fold perspective*. First, to better capitalize dumb sensors, we optimized the system detection performance (namely, the non-centrality parameter) by tuning each sensor quantizer via PSOA. Secondly, asymptotic performance allowed to define detection gains (ADG and ANDG) to assess performance improvement arising from the use of additional dumb sensors and from increasing their resolution, as a useful designers' tool. It was shown through simulations that the Rao test, in addition to being asymptotically equivalent to the GLRT, achieves practically the same performance in the
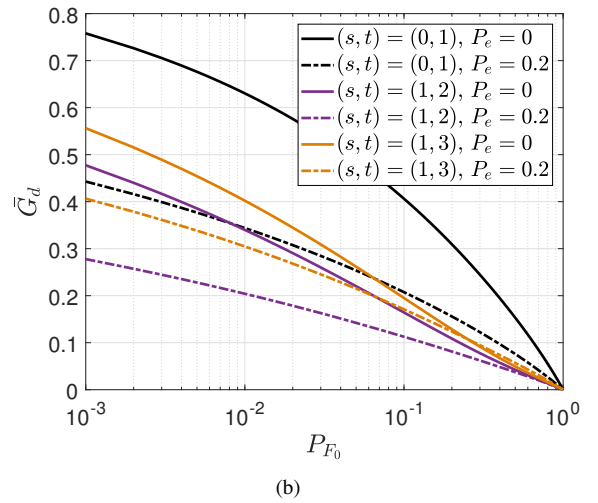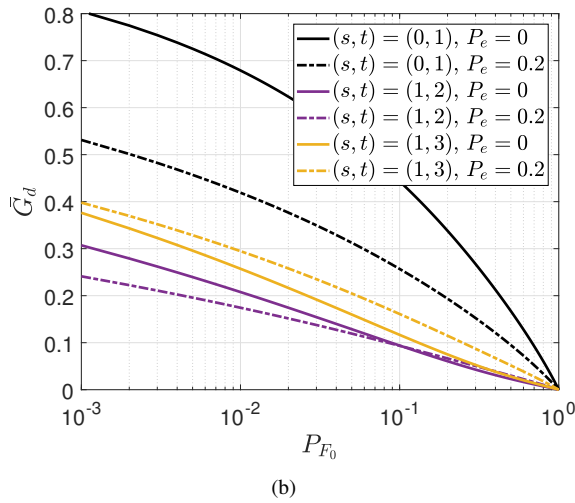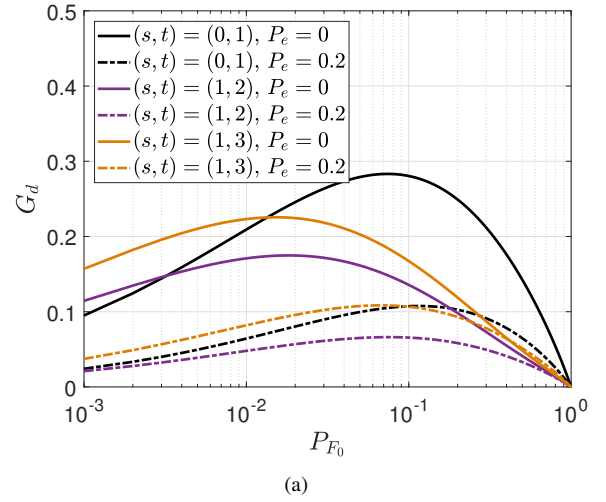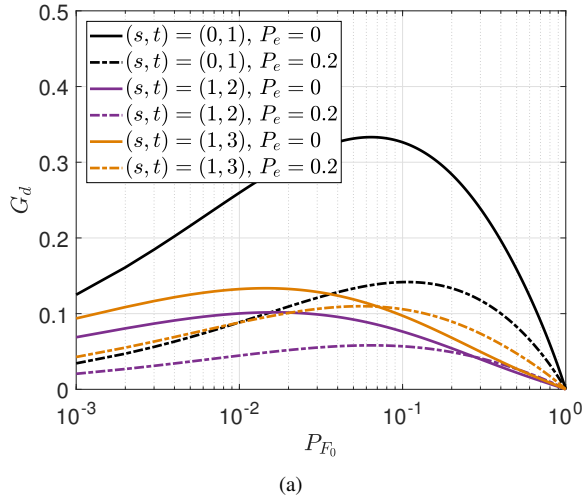
(a)

(b)

Fig. 7: (a): ADG (viz. G_d vs. P_{F_0}) and (b): ANDG (viz. $\bar{G}_d$ vs. P_{F_0}) for a homogeneous WSN with $w_k \sim \mathcal{N}\left(0, \sigma_w^2\right)$, $P_e \in \{0, 0.2\}$ and different configurations (s, t).

(a)

(b)

Fig. 8: (a): ADG (viz. G_d vs. P_{F_0}) and (b): ANDG (viz. $\bar{G}_d$ vs. P_{F_0}) for a homogeneous WSN with $w_k \sim \mathcal{GN}\left(0, \alpha, 3\right)$, $P_e \in \{0, 0.2\}$ and different configurations (s, t).

finite number of sensors case. In addition, results also demonstrated the advantage of multi-bit quantization against one-bit quantization and that a few quantization bits are sufficient to approach with negligible gap the performance of a WSN using only smart sensors in the case of perfect reporting channels. Differently, the presence of errors on the reporting phase increases the performance gap with the unquantized benchmark.

Further directions will include design of Rao test for alternative, more general and realistic measurement & channel models: (a) unknown random signal parameters [26], (b) vector measurement models [39], (c) incompletely specified noise PDFs (e.g. unknown variance [40]), (d) models enjoying sparsity [27], (e) energy-efficient censoring sensors [41] and (f) time-correlated reporting channels [42]. Additionally, the validation of the proposed Rao fusion rule on experimental data, to assess the sensitivity to model mismatch, is of clear interest and left to future work. Finally, optimization of the number of dumb & smart sensors subject to both (i) communication and (ii) performance budgets [43], [44] will be also

considered as a future study.

APPENDIX A
PROOF OF EQ. (11) (SCORE FUNCTION)

Based on the factorization form in (4), the log-likelihood function $p\left(\boldsymbol{Y}, \boldsymbol{s}; \theta\right)$ is given by

$$\ln[p\left(\boldsymbol{Y}, \boldsymbol{s}; \theta\right)] = \tag{33}$$
$$\sum_{k=1}^{K_q} \ln P\left(\boldsymbol{y}_k; \theta\right) + \sum_{\kappa=1}^{K_u} \ln p_{w_{K_q+\kappa}} \left(s_\kappa - h_{K_q+\kappa}\theta\right)$$

For notational convenience, we then define $L_{\boldsymbol{Y}}(\theta) \triangleq \sum_{k=1}^{K_q} \ln P\left(\boldsymbol{y}_k; \theta\right)$ and $L_{\boldsymbol{s}}(\theta) \triangleq \sum_{\kappa=1}^{K_u} \ln p_{w_{K_q+\kappa}}(s_\kappa - h_{K_q+\kappa}\theta)$, respectively. Accordingly, the derivatives of $L_{\boldsymbol{Y}}(\theta)$

and $L_{\boldsymbol{s}}(\theta)$ with respect to θ can be written respectively as

$$\frac{\partial L_{\boldsymbol{Y}}(\theta)}{\partial \theta} = \sum_{k=1}^{K_q} \frac{P'(\boldsymbol{y}_k; \theta)}{P(\boldsymbol{y}_k; \theta)} \tag{34}$$

$$= \sum_{k=1}^{K_q} \frac{h_k \sum_{i=1}^{2^{q(k)}} P(\boldsymbol{y}_k | \boldsymbol{b}_k = \boldsymbol{v}(i)) \rho(\boldsymbol{b}_k = \boldsymbol{v}(i); \theta)}{\sum_{i=1}^{2^{q(k)}} P(\boldsymbol{y}_k | \boldsymbol{b}_k = \boldsymbol{v}(i)) P(\boldsymbol{b}_k = \boldsymbol{v}(i); \theta)},$$

and

$$\frac{\partial L_{\boldsymbol{s}}(\theta)}{\partial \theta} = -\sum_{\kappa=1}^{K_u} \frac{h_{K_q+\kappa} \, p'_{w_{K_q+\kappa}} (s_\kappa - h_{K_q+\kappa}\theta)}{p_{w_{K_q+\kappa}} (s_\kappa - h_{K_q+\kappa}\theta)}, \tag{35}$$

where $P'(\boldsymbol{y}_k; \cdot)$ and $p'_{w_{K_q+\kappa}}(\cdot)$ denote the derivative of $P(\boldsymbol{y}_k; \cdot)$ and $p_{w_{K_q+\kappa}}(\cdot)$, respectively. Additionally, in Eq. (34) we have exploited the definition:

$$\rho(\boldsymbol{b}_k = \boldsymbol{v}(i); \theta) \triangleq p_{w_k}(\tau_k(i-1) - h_k\theta) - p_{w_k}(\tau_k(i) - h_k\theta) \tag{36}$$

As a consequence, gathering the above results, we obtain

$$\frac{\partial \ln[p(\boldsymbol{Y}, \boldsymbol{s}; \theta)]}{\partial \theta} = \frac{\partial L_{\boldsymbol{Y}}(\theta)}{\partial \theta} + \frac{\partial L_{\boldsymbol{s}}(\theta)}{\partial \theta}$$

$$= \sum_{k=1}^{K_q} \frac{h_k \sum_{i=1}^{2^{q(k)}} P(\boldsymbol{y}_k | \boldsymbol{b}_k = \boldsymbol{v}(i)) \rho(\boldsymbol{b}_k = \boldsymbol{v}(i); \theta)}{\sum_{i=1}^{2^{q(k)}} P(\boldsymbol{y}_k | \boldsymbol{b}_k = \boldsymbol{v}(i)) P(\boldsymbol{b}_k = \boldsymbol{v}(i); \theta)} \tag{37}$$

$$- \sum_{\kappa=1}^{K_u} \frac{h_{K_q+\kappa} \, p'_{w_{K_q+\kappa}} (s_\kappa - h_{K_q+\kappa}\theta)}{p_{w_{K_q+\kappa}} (s_\kappa - h_{K_q+\kappa}\theta)}$$

Finally, based on Eq. (37), the desired result in (11) is obtained by simple squaring operation. This concludes the proof.

APPENDIX B
PROOF OF EQ. (12) (FISHER INFORMATION)

Since the measurements among the sensors are independent, the FI with respect to the parameter θ can be rewritten as follows

$$I(\theta) \triangleq \mathbb{E}_{\{\boldsymbol{Y}, \boldsymbol{s}\}} \left\{ \left(\frac{\partial \ln[p(\boldsymbol{Y}, \boldsymbol{s}; \theta)]}{\partial \theta} \right)^2 \right\} \tag{38}$$

$$= \mathbb{E}_{\{\boldsymbol{Y}, \boldsymbol{s}\}} \left\{ \left(\frac{\partial L_{\boldsymbol{Y}}(\theta)}{\partial \theta} + \frac{\partial L_{\boldsymbol{s}}(\theta)}{\partial \theta} \right)^2 \right\} \tag{39}$$

$$= \underbrace{\mathbb{E}_{\boldsymbol{Y}} \left\{ \left(\frac{\partial L_{\boldsymbol{Y}}(\theta)}{\partial \theta} \right)^2 \right\}}_{\triangleq I_q(\theta)} + \underbrace{\mathbb{E}_{\boldsymbol{s}} \left\{ \left(\frac{\partial L_{\boldsymbol{s}}(\theta)}{\partial \theta} \right)^2 \right\}}_{\triangleq I_u(\theta)} \tag{40}$$

that is, we can express the FI as the result of *two terms*, the first due to dumb sensors (viz. $I_q(\theta)$) and the second due to smart sensors (viz. $I_u(\theta)$).

The *first* term can be obtained by directly resorting to the result for quantized measurements in [26], which provides $I_q(\theta)$ in closed form as

$$I_q(\theta) = \tag{41}$$

$$\sum_{k=1}^{K_q} h_k^2 \sum_{i=1}^{2^{q(k)}} \frac{\left\{ \sum_{j=1}^{2^{q(k)}} G_{q(k)}(P_{e,k}, d_{i,j}) \rho(\boldsymbol{b}_k = \boldsymbol{v}(j); \theta) \right\}^2}{\sum_{j=1}^{2^{q(k)}} G_{q(k)}(P_{e,k}, d_{i,j}) P(\boldsymbol{b}_k = \boldsymbol{v}(j); \theta)},$$

where the definition in Eq. (36) has been again exploited. We highlight that the additive form in Eq. (41) directly follows from independence of sensors (multi-bit) decisions.

On the other hand, it can be easily shown that the *second term* $I_u(\theta)$ has the form (exploiting smart sensors' independence)

$$I_u(\theta) = I_u = \sum_{\kappa=1}^{K_u} h_{K_q+\kappa}^2 \, I_{w_{K_q+\kappa}}, \tag{42}$$

where $I_{w_{K_q+\kappa}} \triangleq \int [\partial \ln p_{w_{K_q+\kappa}}(\zeta)/\partial\zeta]^2 \, p_{w_{K_q+\kappa}}(\zeta) \, d\zeta$. The latter term appears to have a very simple form in many cases of interest, such as $w_k \sim \mathcal{N}(0, \sigma_w^2)$ (equal to $1/\sigma_w^2$), $w_k \sim \mathcal{L}(0, \beta)$ (equal to $1/\beta^2$) and $w_k \sim \mathcal{GN}(0, \alpha, \epsilon)$ (equal to $(1/\alpha^2)\,[\epsilon(\epsilon-1)\,\Gamma(1-1/\epsilon)]/\Gamma(1/\epsilon))$ [45]. Finally, combining (41) and (42), the FI can be written as in Eq. (12). This concludes the proof.

REFERENCES

[1] J. N. Tsitsiklis, "Decentralized detection," *Advances in Statistical Signal Processing*, vol. 2, no. 2, pp. 297–344, 1993.

[2] R. Viswanathan and P. K. Varshney, "Distributed detection with multiple sensors - Part I: Fundamentals," *Proc. IEEE*, vol. 85, no. 1, pp. 54–63, Jan. 1997.

[3] R. S. Blum, S. A. Kassam, and H. V. Poor, "Distributed detection with multiple sensors II. Advanced topics," *Proc. IEEE*, vol. 1997, no. 1, pp. 64–79, Jan. 1997.

[4] I. F. Akyildiz, W. Su, Y. Sankarasubramaniam, and E. Cayirci, "A survey on sensor networks," *IEEE Commun. Mag.*, vol. 40, no. 8, pp. 102–114, Aug 2002.

[5] J.-J. Xiao and Z.-Q. Luo, "Decentralized estimation in an inhomogeneous sensing environment," *IEEE Trans. Inf. Theory*, vol. 51, no. 10, pp. 3564–3575, Oct 2005.

[6] R. Niu and P. K. Varshney, "Joint detection and localization in sensor networks based on local decisions," in *Fortieth Asilomar Conference on Signals, Systems and Computers*, 2006, pp. 525–529.

[7] B. Chen, L. Tong, and P. K. Varshney, "Channel-aware distributed detection in wireless sensor networks," *IEEE Signal Process. Mag.*, vol. 23, no. 4, pp. 16–26, Jul. 2006.

[8] T. Wu and Q. Cheng, "Distributed estimation over fading channels using one-bit quantization," *IEEE Trans. Wireless Commun.*, vol. 8, no. 12, pp. 5779–5784, 2009.

[9] D. Ciuonzo, G. Romano, and P. Salvo Rossi, "Channel-aware decision fusion in distributed MIMO wireless sensor networks: Decode-and-fuse vs. decode-then-fuse," *IEEE Trans. Wireless Commun.*, vol. 11, no. 8, pp. 2976–2985, Aug. 2012.

[10] S. Kar, H. Chen, and P. K. Varshney, "Optimal identical binary quantizer design for distributed estimation," *IEEE Trans. Signal Process.*, vol. 60, no. 7, pp. 3896–3901, 2012.

[11] D. Ciuonzo and P. Salvo Rossi, "Quantizer design for generalized locally-optimum detectors in wireless sensor networks," *IEEE Wireless Commun. Lett.*, vol. 7, no. 2, pp. 162–165, Apr. 2018.

[12] D. Li, K. D. Wong, Y. H. Hu, and A. M. Sayeed, "Detection, classification, and tracking of targets," *IEEE Signal Process. Mag.*, vol. 19, no. 2, pp. 17–29, Mar 2002.

[13] M. N. Kurt and X. Wang, "Multi-sensor sequential change detection with unknown change propagation pattern," *IEEE Trans. Aerosp. Elect. Syst.*, 2018.

[14] S. Nallagonda, S. D. Roy, S. Kundu, G. Ferrari, and R. Raheli, "Censoring-based cooperative spectrum sensing with improved energy detectors and multiple antennas in fading channels," *IEEE Trans. Aerosp. Elect. Syst.*, vol. 54, no. 2, pp. 537–553, 2018.

[15] R. Palamà, M. S. Greco, and F. Gini, "Multistatic adaptive CFAR detection in non-Gaussian clutter," *EURASIP Journal on Advances in Signal Processing*, vol. 2016, no. 1, p. 107, 2016.

[16] A. M. Haimovich, R. S. Blum, and L. J. Cimini, "MIMO radar with widely separated antennas," *IEEE Signal Process. Mag.*, vol. 25, no. 1, pp. 116–129, 2008.

[17] C. Y. Chong, F. Pascal, J.-P. Ovarlez, and M. Lesturgie, "MIMO radar detection in non-Gaussian and heterogeneous clutter," *IEEE J. Sel. Topics Signal Process.*, vol. 4, no. 1, pp. 115–126, 2010.

[18] J. Fang and H. Li, "Distributed estimation of Gauss-Markov random fields with one-bit quantized data," *IEEE Signal Process. Lett.*, vol. 17, no. 5, pp. 449–452, May 2010.

[19] J. Fang, Y. Liu, H. Li, and S. Li, "One-bit quantizer design for multisensor GLRT fusion," *IEEE Signal Process. Lett.*, vol. 20, no. 3, pp. 257–260, Mar. 2013.

[20] A. R. Reibman and L. L. W. Nolte, "Optimal detection and performance of distributed sensor systems," *IEEE Trans. Aerosp. Electron. Syst.*, no. 1, pp. 24–30, 1987.

[21] I. Y. Hoballah and P. K. Varshney, "Distributed Bayesian signal detection," *IEEE Transactions on Information Theory*, vol. 35, no. 5, pp. 995–1000, 1989.

[22] D. Ciuonzo, G. Papa, G. Romano, P. Salvo Rossi, and P. Willett, "One-bit decentralized detection with a Rao test for multisensor fusion," *IEEE Signal Process. Lett.*, vol. 20, no. 9, pp. 861–864, Sept 2013.

[23] D. Ciuonzo, G. Romano, and P. Salvo Rossi, "Optimality of received energy in decision fusion over Rayleigh fading diversity MAC with non-identical sensors," *IEEE Trans. Signal Process.*, vol. 61, no. 1, pp. 22–27, Jan. 2013.

[24] C. A. M. Sotomayor, R. P. David, and R. Sampaio-Neto, "Adaptive nonassisted distributed detection in sensor networks," *IEEE Trans. Aerosp. Elect. Syst.*, vol. 53, no. 6, pp. 3165–3174, 2017.

[25] F. Gao, L. Guo, H. Li, and J. Fang, "One-bit quantization and distributed detection with an unknown scale parameter," *MDPI Algorithms*, vol. 8, no. 3, pp. 621–631, 2015.

[26] F. Gao, L. Guo, H. Li, J. Liu, and J. Fang, "Quantizer design for distributed GLRT detection of weak signal in wireless sensor networks," *IEEE Trans. Wireless Commun.*, vol. 14, no. 4, pp. 2032–2042, April 2015.

[27] H. Zayyani, F. Haddadi, and M. M. Korki, "Double detector for sparse signal detection from one-bit compressed sensing measurements," *IEEE Signal Process. Lett.*, vol. 23, no. 11, pp. 1637–1641, 2016.

[28] R. C. Farias, E. Moisan, and J.-M. Brossier, "Optimal asymmetric binary quantization for estimation under symmetrically distributed noise," *IEEE Signal Process. Lett.*, vol. 21, no. 5, pp. 523–526, 2014.

[29] G. Wang, J. Zhu, and Z. Xu, "Asymptotically optimal one-bit quantizer design for weak-signal detection in generalized Gaussian noise and lossy binary communication channel," *Elsevier Signal Processing*, vol. 154, pp. 207–216, 2019.

[30] S. Li, X. Li, X. Wang, and J. Liu, "Decentralized sequential composite hypothesis test based on one-bit communication." *IEEE Trans. Inf. Theory*, vol. 63, no. 6, pp. 3405–3424, 2017.

[31] D. Ciuonzo, P. Salvo Rossi, and P. Willett, "Generalized Rao test for decentralized detection of an uncooperative target," *IEEE Signal Process. Lett.*, vol. 24, no. 5, pp. 678–682, 2017.

[32] A. Ribeiro and G. B. Giannakis, "Bandwidth-constrained distributed estimation for wireless sensor networks - Part I: Gaussian case," *IEEE Trans. Signal Process.*, vol. 54, no. 3, pp. 1131–1143, Mar. 2006.

[33] A. I. F. Vaz and L. N. Vicente, "A particle swarm pattern search method for bound constrained global optimization," *Journal of Global Optimization*, vol. 39, no. 2, pp. 197–219, 2007.

[34] D. Saska, R. S. Blum, and L. Kaplan, "Fusion of quantized and unquantized sensor data for estimation," *IEEE Signal Process. Lett.*, vol. 22, no. 11, pp. 1927–1930, Nov 2015.

[35] N. Harel and T. Routtenberg, "Non-Bayesian estimation with partially quantized observations," in *22nd IEEE International Conference on Digital Signal Processing (DSP)*, 2017, pp. 1–5.

[36] S. M. Kay, *Fundamentals of Statistical Signal Processing, Volume 2: Detection Theory*. Prentice Hall PTR, Jan. 1998.

[37] X. Cheng, D. Ciuonzo, and P. Salvo Rossi, "Multi-bit decentralized detection of a weak signal in wireless sensor networks with a Rao test," in *IEEE International Conference on Digital Signal Processing (DSP)*, 2018, pp. 1–5.

[38] M. Clerc, *Particle swarm optimization*. John Wiley & Sons, 2010, vol. 93.

[39] J. Fang, X. Li, H. Li, and L. Huang, "Precoding for decentralized detection of unknown deterministic signals," *IEEE Trans. Aerosp. Elect. Syst.*, vol. 50, no. 3, pp. 2116–2128, July 2014.

[40] A. De Maio and S. Iommelli, "Coincidence of the Rao test, Wald test, and GLRT in partially homogeneous environment," *IEEE Signal Process. Lett.*, vol. 15, pp. 385–388, 2008.

[41] C. Rago, P. Willett, and Y. Y. Bar-Shalom, "Censoring sensors: A low-communication-rate scheme for distributed detection," *IEEE Trans. Aerosp. Elect. Syst.*, vol. 32, no. 2, pp. 554–568, 1996.

[42] N. Biswas, P. Ray, and P. K. Varshney, "Distributed detection over channels with memory," *IEEE Signal Process. Lett.*, vol. 22, no. 12, pp. 2494–2498, 2015.

[43] C.-Y. Yu and P. K. Varshney, "Bit allocation for discrete signal detection," *IEEE Trans. Commun.*, vol. 46, no. 2, pp. 173–175, 1998.

[44] Q. Cheng, P. K. Varshney, K. G. Mehrotra, and C. K. Mohan, "Bandwidth management in distributed sequential detection," *IEEE Trans. Inf. Theory*, vol. 51, no. 8, pp. 2954–2961, Aug 2005.

[45] S. Nadarajah, "A generalized normal distribution," *Journal of Applied Statistics*, vol. 32, no. 7, pp. 685–694, 2005.

Xu Cheng was born on October 30th, 1987. He received the B.Sc. degree in communication engineering, the M.Sc. and the Ph.D. degrees in information and communication engineering, respectively, in 2009, 2011 and 2016, from the National University of Defense Technology, Changsha, China.

From October 2014 to October 2015, he was a visiting student with the University of Naples "Federico II", Naples, Italy. He is currently working as an assistant professor at the College of Armed Police, Chengdu, China. His research interests concentrate on statistical signal processing, with emphasis on the application of radar systems and wireless sensor networks (WSNs).

Domenico Ciuonzo (S'11-M'14-SM'16) is currently an Assistant Professor at University of Napoli Federico II, Italy. He holds a Ph.D. in Electronic Engineering from University of Campania "L. Vanvitelli", Italy and, from 2011, he has held several visiting researcher appointments. Since 2014 he is editor of several IEEE, IET and ELSEVIER journals. His research interests include data fusion, statistical signal processing, wireless sensor networks, Internet of Things, traffic analysis and machine learning.
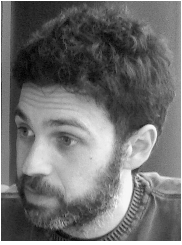
Pierluigi Salvo Rossi was born in Naples, Italy, on April 26, 1977. He received the Doctor Engineering degree in telecommunications engineering (summa cum laude) and the PhD degree in computer engineering, in 2002 and 2005, respectively, both from the University of Naples "Federico II", Italy. From 2005 to 2008, he worked as a postdoc at the Dept. Computer Science and Systems, University of Naples "Federico II", Italy, at the Dept. Information Engineering, Second University of Naples, Italy, and at the Dept. Electronics and Telecommunications, Norwegian University of Science and Technology (NTNU), Trondheim, Norway. From 2008 to 2014, he was an assistant professor (tenured in 2011) in telecommunications with the Dept. Industrial and Information Engineering, Second University of Naples, Italy. From 2014 to 2016, he was an associate professor in signal processing with the Dept. Electronics and Telecommunications, NTNU, Norway. From 2016 to 2017, he was a full professor in signal processing with the Dept. Electronic Systems, NTNU, Norway. From 2017 to 2019, he was a principal engineer with the Dept. Advanced Analytics and Machine Learning Team, Kongsberg Digital AS, Trondheim, Norway. Since 2019 he is a full professor in signal processing with the Dept. Electronic Systems, NTNU, Norway. He held visiting appointments at the Dept. Electrical and Computer Engineering, Drexel University, Philadelphia, PA, US, at the Dept. Electrical and Information Technology, Lund University, Sweden, at the Dept. Electronics and Telecommunications, NTNU, Norway, and at the Excellence Center for Wireless Sensor Networks, Uppsala University, Sweden.

He is an IEEE senior member and serves as an area editor for the IEEE Open Journal of the Communications Society (since 2019), a senior editor for the IEEE Communication Letter (since 2016), an associate editor for the IEEE Transactions on Signal and Information Processing over Networks (since 2019) and an associate editor for the IEEE Transactions on Wireless Communication (since 2015). He was an associate editor for the IEEE Communication Letter (from 2012 to 2016) and a Guest Editor for Elsevier Physical Communication. (2012). His research interests fall within the areas of communications, machine learning, and signal processing.